IEEE Access
Multidisciplinary | Rapid Review | Open Access Journal

Received November 3, 2018, accepted November 15, 2018, date of publication December 5, 2018,
date of current version December 31, 2018.

Digital Object Identifier 10.1109/ACCESS.2018.2885087

Experimental Breast Phantoms for Estimation of Breast Tumor Using Microwave Imaging Systems

MD TARIKUL ISLAM, MD SAMSUZZAMAN, (Member, IEEE), SALEHIN KIBRIA, AND MOHAMMAD TARIQUL ISLAM, (Senior Member, IEEE)
Center of Advanced Electronic and Communication Engineering, Universiti Kebangsaan Malaysia, Bangi 43600, Malaysia

Corresponding authors: Md Tarikul Islam (P94299@siswa.ukm.edu.my), Md Samsuzzaman (samsuzzaman@ukm.edu.my), and Mohammad Tariqul Islam (tariqul@ukm.edu.my)

This work is supported by the University Research Grant under the Project code: MI-2017-001.

ABSTRACT In this paper, the preparation and the measurement of a set of human breast phantoms for microwave breast imaging (MBI) as a method of tumor detection are presented. The developed artificial breast phantoms have realistic dielectric properties. Homogenous and most realistic heterogeneous breast phantoms have been fabricated based upon 3D structures filled up with different chemical mixtures that imitate the various breast tissue types (skin, healthy fat tissue, glandular tissue, and tumor tissue) regarding permittivity over ultra-wideband frequency band (3.1–10.6 GHz). The primary challenge in fabricating such phantoms is in developing suitable mixtures of materials to emulate those properties across the frequency band of interest in hyperthermia and to fabricate the phantom with realistic anatomy. Once fabricated, the dielectric properties are measured using a dielectric probe connected with a modern vector network analyzer. The measured dielectric is compared to real human breast dielectric properties, and the primary imaging results are presented. The integrated design of the homogenous and heterogeneous phantoms permits to combine the tumor and breast phantoms dynamically for creating a test platform based on MBI systems. The experimental dielectric properties of the phantoms show good agreement with this paper and theoretical results. The phantoms are constructed in such a way that the chosen materials demonstrate the properties to be stable over a long period. The experimental results demonstrate the validity of our proposed phantoms to be used in investigating as a supplement to the real human breast tissue with multiple object and comparatively high-resolution image.

INDEX TERMS Microwave imaging, breast phantom, dielectric properties, homogenous phantom, heterogenous phantom.

I. INTRODUCTION

Microwave imaging is considered as the promising technique for medical applications, like cancer (tumor) detection in human breasts from several years. There has been immense progress in research activity in microwave diagnostics and healing technologies targeting the breast for over the past two decades [1]–[6]. These investigations have been powered by the clinical needs for inventory tools in early detection of breast tumor at low cost and nonionizing features of microwave systems. This is a promising and essential prospect to develop tomographic systems for the finding of a breast tumor. The breast tumor is the prominent cause of cancer among women [7]. Novel technologies for detecting and diagnosis could lessen the rate of death across the world. For significant survival, early detection and treatment can be the compelling solution. The tumor showed significantly high dielectric constant rather than normal healthy tissues [8] in various range of microwave frequencies. It becomes the key feature for better detection abilities with microwave techniques over the existing X-ray mammography and ultrasound imaging. Hereafter, several experimental systems [3]–[5], as well as algorithms for imaging [5], [9]–[13], have been proposed and promising results have been gained for radar-based [4] and reverse scattering image renovation algorithms [9]. For testing the performance stability, resolution and Point Spread Function (PSF), the effect of experimental

errors and noise in algorithmic performance and accuracy of new devices, systems, and algorithms, which associated to microwave breast tumor detection system, breast phantoms with high fidelity, are complementary tools for experimental and computational investigations. The proper breast phantom can precisely impersonators not only the 3D dispersal of different layers of breast tissues (skin, fat, glandular, tumor) but also explicit the physical characteristics of those tissues applicable to microwave collaborations with the phantom. Laboratory phantoms can play a vital role in quality insurance of clinical MBI systems, comply with the common practice of existing imaging technologies [10].

Phantoms are artificial replicas of body organs or parts premeditated to mock the structure and physical assets of their organic matching parts. Permittivity and conductivity are the interesting parameters besides the geometry in microwave tomography. The materials previously used as a tissue substitute are liquid glycerin [11], rubber-carbon mix [12] and Triton X-100 [13]. A human breast can be classified into two primary parts, adipose and fibro-glandular tissue, that can be eminent to each other by unique properties of dielectric due to corresponding water, fat and protein content [14]. To match the dielectric properties, different mixture recipe has been proposed leaving substantial argument as to which values are most appropriate to use in experimental systems. In [15], the permittivity was reported as 45, 25 and 7 for malignant, fibro-glandular and fat tissues respectively at 1.5 GHz. More sophisticated phantoms were developed by Burfeindt *et al.* [16], Joachimowicz *et al.* [17] and by Pistorius *et al.* [18] at the University of Manitoba. Several experimental phantoms for MBI systems are stated in the literature [12], [17], [19]–[21]. One of the recent methods is constructed on the zero-order mode resonator structure of metamaterial [22], [23]. Guy [24] developed the first gel-based phantom where TX-150 is the base ingredient for the simulation of high water-containing tissues along with polyethylene powder and saline solution. Lazebnik *et al.* [19] proposed an alternative phantom made with water, gelatin, kerosene and sunflower oil for the frequency range of 500 MHz–20 GHz. Agar-based phantoms were designed by Kato and Ishida for hyperthermia for the first time [25] to test RF hyperthermia at 13.56 MHz that is the combination of water (97.57%), NaCl (0.43%) and agar powder (2%). Agar phantoms are appropriated for using in the applications at higher temperatures for its high melting point (80°C approx.) like hyperthermia and ablation [26]. Mostly the available phantoms are different from tissue mimicking material (TMM) which is responsible for the recreation of breast tissue properties. The breast skin shape also differs from some proposed studies that work on MRI driven and 3D-printed shells that represent the skin anatomically. With the various shape and inner structures, oil-gelatin based breast phantom has been fabricated in [19] and [27] where the different mixing percentage of oil control the dielectric properties. The main drawback of this phantom is very subtle to an environmental acquaintance and short lifetime.

The TMM phantoms based on Triton X-100 have been proposed in [13] and [20] whereby varying the amount of raw materials the dielectric is controlled and is more stable in higher temperature than oil-gelatin mixtures. There is a significant drawback of liquid-based phantoms [16], [17] as internal and external shells are used to form the anatomy of the breast which has a significant effect on the fidelity of the backscattered signals received from MBI systems. Nevertheless, the recent experiments have not involved the most realistic tumor model, which is prerequisite for any kind of study related to diagnosis. Tumor models have been considered as ellipsoidal or spherical targets and used numerical simulations that can lead the noisy experiment data while collecting backscattering signals in MBI examination [28], [29].

In this paper, the development of novel homogenous and most realistic heterogeneous tumor phantom with different sizes is presented. Polyethylene and agar-based two layers (fat and tumor) homogenous phantom and agar-Xanthium based four layers (skin, fat, gland and tumor) are fabricated. The dielectric properties are measured for each layer, and a 3D shape with complex real human-like construction is given for making the phantom more suitable for the experiment of MBI system. The primary result of imaging with the MBI system of the phantoms is also investigated.

II. ELECTROMAGNETIC PROPERTIES OF BREAST PHANTOM

The study of the electromagnetic depiction of normal and malicious human breast tissues has been focused over the years. For being complex compositions, the large-scale investigation covering wider frequency band has not been carried out before Lazebnik *et al.* [30] reported the verity of dielectric properties of heterogeneous phantoms especially the normal breast tissues depending on the concentration of adipose tissue content. Also, the variability of the properties of malignant tissues also stated by the authors for the same reasons. The dielectric properties of several types of tissues are categorized by permittivity, which is the mean of complex-valued dielectric,

$$\varepsilon\ (\varepsilon = \varepsilon_r + i\sigma/\omega\varepsilon_0) \tag{1}$$

where εr represents the dielectric constant and σ represents the conductivity of the tissue against frequency. γ_0 is the vacuum dielectric permittivity, and ω is angular frequency. The evaluation of the described Debye model is considered under the frequency range 0.5 to 6 GHz [31].

A. DIELECTRIC PROPERTIES OF BREAST TISSUES

The comprehensive study of dielectric properties of healthy and malignant tissues in large scale was conducted by Lazebnik *et al.* [30], [32] in 2007. The heterogenous complex internal structure found in breast tissue where a few amounts of contrast relay between healthy and malignant

TABLE 1. The dielectric properties (εr and σ) for four breast tissues: skin, fat, gland and tumor, with targeted dielectric at 3 GHz frequency.

	Skin		Fat		Gland		Tumor	
	ε_r	σ(S/m)	ε_r	σ(S/m)	ε_r	σ(S/m)	ε_r	σ(S/m)
Target [30, 32]	38	1.8	5	0.1	47	2.1	67	3.1
Triton-X-100 [17]	-	-	5	0.1	35-46	1.4-2.0	52	2.1
Oil-gelatin [27]	38	1.6	7	0.2	38-48	1.6-2.0	-	-
Oil-gelatin [36]	36	2	13	0.6	32	1.4	54	2.5
Rubber solid [37]	24	1.6	5	0.2	36	3.0	>36	>3.0

tissues. However, the recent clinical experiments recommend that there is significant healthy-to-cancerous contrast ratio [33]–[35]. The properties stated in [32] is still considered as the targeted properties of the breast development for both homogeneous and heterogeneous phantoms which also characterize in a worst-case scenario. The median target relative permittivity and conductivity of fat, glandular, skin and tumor tissues are displayed in Table 1.

The dielectric properties (εr and σ) for four breast tissues: skin, fat, gland and tumor, with targeted dielectric at 3 GHz frequency is summarized in Table 1.

B. FABRICATION PROTOCOL

Two types of phantoms are fabricated as homogeneous and heterogeneous phantoms. The homogenous phantom has skin layer, fatty layer and a tumor inside. The heterogeneous phantom has a skin layer, a fatty layer, gland and tumors inside. Two different methods are used in constructing the two phantoms. For homogenous phantom, Sodium chloride (NaCl), polyethylene powder, agar powder, xanthan gum, sodium dehydroacetate monohydrate, and distilled water are used. Polyethylene powder is used to adjust the permittivity and NaCl to improve the conductivity. Agar is used to maintaining the shape of the phantom by preventing separation of water content, xanthan gum is used as a thickener and sodium dehydroacetate monohydrate as a preservative. The materials which alter the dielectric properties of this method are NaCl, polyethylene powder, agar, and distilled water, and they are the main ingredients in the phantom. For heterogeneous phantom, distilled water, safflower oil, propylene glycol, 200 bloom calf-skin gelatin, formalin (37% formaldehyde solution) and surfactant (xanthan gum) are used. Propylene glycol and safflower oil are used because they have low conductivity suitable to create a low conductivity phantom and high permittivity property of distilled water appropriate to increase the permittivity of the phantom. Gelatin mixtures have dielectric properties very close to the breast tissues dielectric property and are stable enough to last up to 8 weeks [13]. These materials are also natural to fabricate and possess high mechanical properties. The selected materials make it easy to produce breast phantoms although different concentrations of the materials are used for different layers. The table 2 and table 3 below shows the equivalent amount of all the materials used in making both the homogenous and heterogeneous phantom, respectively.

TABLE 2. The composition of the homogeneous phantom.

Material	Quantity		Purpose
	Fatty phantom	Tumor	
Distilled water	420 ml	420 ml	Solvent
Polyethylene powder	500g	43g	Modifying electrical permittivity
Agar	20g	20g	Mechanical strength
NaCl	2.3g	28.3g	Modifying electrical conductivity
Xanthan gum	6.25g	6.25g	Thickener
Sodium dehydroacetate monohydrate	0.25g	0.25g	Preservative

C. THE MEASUREMENT METHOD OF DIELECTRIC PROPERTY

The measurement is taken in UWB (3.1-10.6 GHz) frequency range. A dielectric probe from KEYSIGHT modeled as 85070E dielectric probe kit, operated by the 85070-software installed with PNA-L N5232A (300 KHz to 20 GHz), Vector network analyzer (VNA) is used to measure the dielectric constant (Dk) and loss tangent (Tan δ). The probe test is considered as one of the most popular and easy to use the technique to get the dielectric properties [38]–[40], which is considered as a non-destructive test that does not affect measuring substrate with the capability of the probe method measurement up to 20 GHz [41]. First, the probe is calibrated with 25 cm3 of sterile water. Then all the samples of the phantoms are measured at the UWB frequency range. All the samples are sliced separately for ensuring enough contact between the probe and the sample while taking measurements. To access the consistency the visual checkup of the inner part of the individual sample is done. The outer surface is sanded flat for ensuring no gap between the probe and sample. For better accuracy, 5 sample data of each sample are taken at different locations across the surface. The final decision is then made by calculating the mean value. The percentage disparity of the measurements regarding relative permittivity was found to be 4.5% for skin, 3% for fat, 3.5% for glandular tissue, and 2% for tumor tissues. In terms of the conductivity, the percentage error of the measurements is determined to be 2% for skin, 1% for fat, 2.5% for glandular tissue, and 4% for tumor tissues.

TABLE 3. The composition of the heterogeneous phantom.

Material	Quantity				Purpose
	Skin	Fat	Gland	Tumor	
Distilled water	80 ml	40 ml	80 ml	100 ml	Solvent + modification of permittivity
Safflower oil	14 ml	39 ml	21 ml	7 ml	Modification of electric conductivity
Propylene glycol	7 ml	2 ml	7 ml	6.5 ml	Modification of electric conductivity
Agar agar-gelatin powder	5.88g	7g	5g	9g	Maintaining phantom shape by preventing water content separation
Formalin (37% formaldehyde solution)	0.30 ml	0.3 ml	0.3 ml	0.3 ml	Rising melting temperature of agar-gelatin and phantom stabilizing.
Xanthan gum	1.3g	1.3g	1.3g	1.3g	Thickener
Liquid detergent	0.3 ml	0.3 ml	0.3 ml	0.3 ml	Surfactant

III. BREAST PHANTOM DEVELOPMENT

The breast is in direct connection with the surface of the system in most of the current MBI system commercially available now. Therefore, the breast should be conforming to the shape of the prototype during measurement. On the other hand, the experimental valuation of conformal prototype needed the phantoms to be the exact same shape and anatomy of the breast. In this scenario, the authors develop two types of breast phantom, homogenous and heterogeneous phantoms.

A. HOMOGENOUS BREAST PHANTOM FABRICATION

The components and the ratios are followed from table 2 for the preparation of each layer of the homogeneous phantom. The fatty material is prepared by dissolving agar in distilled water, followed by sodium chloride and sodium dehydroacetate monohydrate. After the solution dissolved, it was then heated at a temperature of 80°C and 400W until bubbles started forming and the mixture became transparent. The heat was then turned off, and the solution was poured into a mixer where a certain amount of xanthan gum was added and mixed, followed by polyethylene powder until a uniform mixture is obtained. The mixture was poured into a suitable mold for the anatomical structure and insertion of tumor material into it. While pouring the mold, a straw of 3 mm diameter was inserted into the mold to create a hole for placing the tumor material is shown in figure 2. The tumor material was prepared using the same method but in a different ratio of all the materials used. A little amount of blue color was added to differentiate tumor from the fatty materials. The mold is then kept in the refrigerator for preservation. Figure 3a shows the fatty phantom poured into the mold and figured 3b shows the fatty phantom without tumor outside the mold with the real breast like anatomy. The height of the phantom is 45 mm and radius is 55 mm. The prepared tumor material is shown in figure 3c, and the final homogenous phantom with tumor inserted at a distance of 27.5 mm from the radius with 3 mm diameter is illustrated in figure 3d. Figure 3e and 3f displays the two and four tumors inserted in different locations.

TABLE 4. Dielectric properties of the homogeneous phantom.

Fat tissue						
Properties	Data 1	Data 2	Data 3	Data 4	Data 5	Mean
Permittivity ε_r	8.90	12.91	14.78	13.41	12.89(center)	10.00
Loss tangent	-0.64	-0.58	-0.53	-0.55	-0.50	-0.56
Conductivity (S/m)	2.22	2.91	3.05	2.87	2.51	2.712
Tumor tissue						
Permittivity ε_r	52.36	53.88	58.81	60.97	60.84(center)	57.37
Loss tangent	0.15	0.11	0.25	0.23	0.20	0.19
Conductivity (S/m)	3.06	2.31	5.72	5.46	4.74	4.26

B. HETEROGENEOUS BREAST PHANTOM FABRICATION

The preparation procedure of each layer is similar with different concentration of the materials stated in table 3. Heterogeneous breast phantom was prepared by first mixing propylene glycol with distilled water then placed in a double boiler with the temperature raised to 50°C. Agar and gelatin powder is then added and mixed until it dissolved completely until the mixture turned yellow. At the same time, surfactant and formalin were added to the oil and mixed with the heated solution. The solution of water, propylene glycol and gelatin are removed from the double boiler then stirred until it cools. For further cooling, the solution is placed in the ice bath. Stirring should be done carefully, not vigorously, as air bubbles might appear and affect the dielectric properties. When the mixture reached 25°C, it is placed into containers for molding and refrigerated overnight. For the shaping of the skin layer of the phantom, two equal size bowls are placed at 2 mm gap and hold with three (3) pairs of clips as shown in figure 4. After the skin phantom has solidified, the inner bowl is removed, and the fat layer was added. To place the glandular layer, a portion of the fat at 20mm radius is cut out after it has solidified, and the gland was poured and for the tumors straws

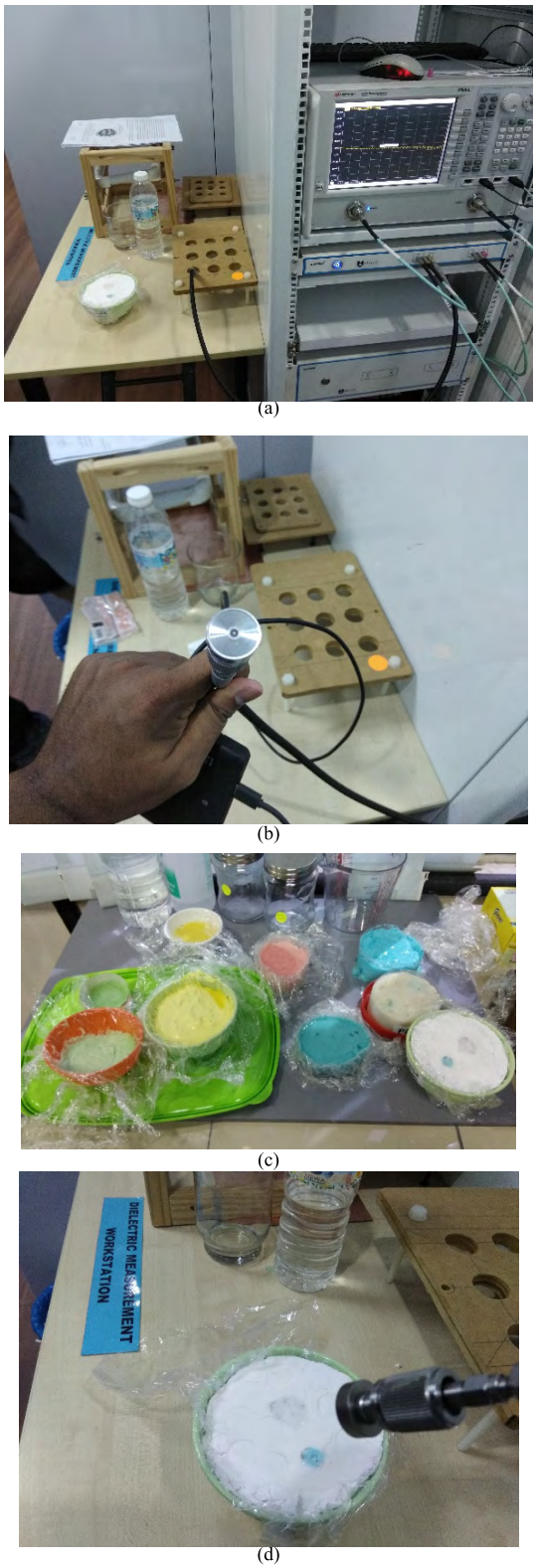

FIGURE 1. Measurement setup of the breast phantom dielectric measurement (a) measurement table and VNA, (b) dielectric probe, (c) phantom samples of different tissues and (d) measurement process.

of different sizes are used to create holes in the gland and then tumor mixture was poured in each hole. To differentiate the layers in the phantom, different food colors are used.

FIGURE 2. Insertion of tumors using straws.

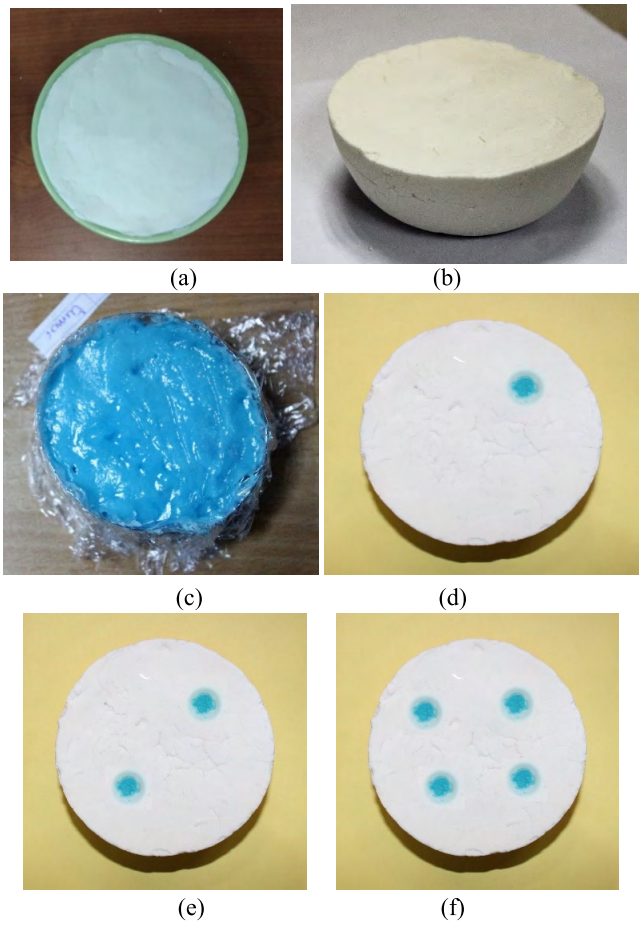

FIGURE 3. Fabricated homogenous phantom (a) phantom poured into a mold, (b) phantom outside the mold without the tumor, (c) separately prepared tumor tissues, (d) complete homogenous phantom with single tumor inserted, (e) phantom with two tumors and (f) phantom with four tumors in a different location.

Figure 5a-d displays the different tissue layers prepared separately for molding and take a measurement. The most realistic and complex anatomic heterogeneous fabricated prototype is shown in figure 6a-c.

FIGURE 4. Setup for preparation of skin layer.

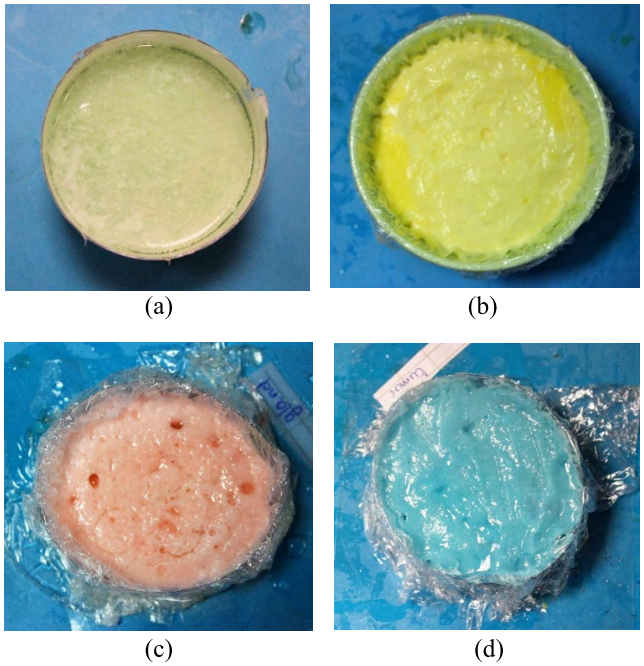

FIGURE 5. Separately prepared four tissue layers (a) skin, (b) fat, (c) gland and (d) tumor.

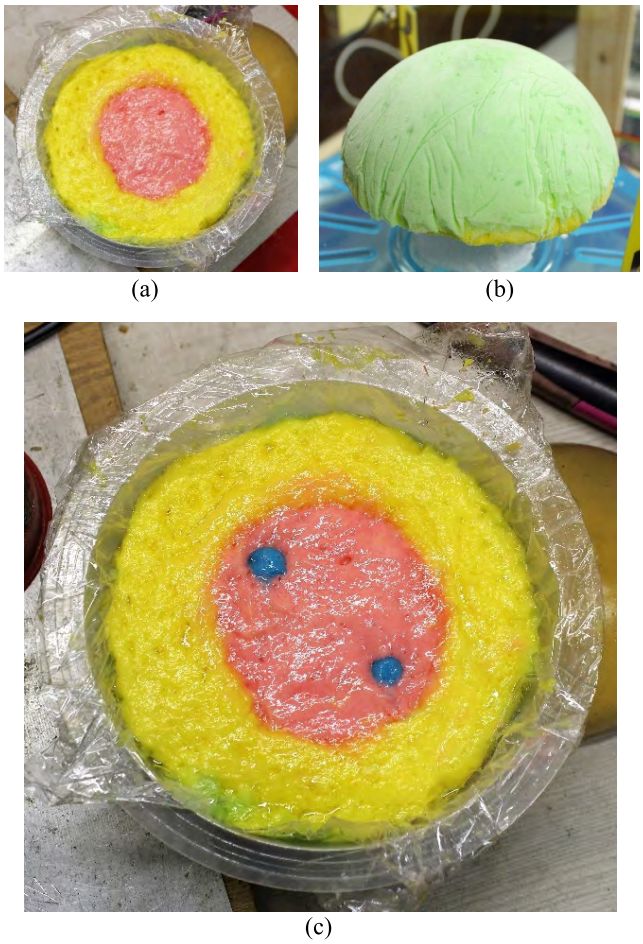

FIGURE 6. Fabricated heterogeneous phantom (a) phantom inside the mold with skin, fat and gland layer, (b) phantom outside the mold, (c) complete phantom with two tumors like material inside.

IV. RESULTS AND DISCUSSIONS

A. DIELECTRIC PROPERTIES OF HOMOGENEOUS PHANTOM

Dielectric properties of the prepared homogenous phantom match the dielectric properties of a real breast together with the targeted one in Table 1. The homogenous phantom was a fatty phantom with a 3mm tumor inside. By using the VNA and probe, five readings are taken at the UWB band (3.1-10.6 GHz), and the measurement is shown here for the center frequency of 7 GHz. The sample data is made in different positions on the surface of the material and then averaged to determine the overall permittivity and conductivity. Table 4 shows the permittivity, loss tangent and conductivity for five sample data and their mean value for the fat and tissue material of the homogeneous phantom. Figure 7a shows the specific relative permittivity for the targeted and measurement results against the UWB frequency band. It is observed a good agreement between the focused and experimental data, which guarantee the appropriateness of the phantoms for testing in MBI systems as a supplement of real suspect. For the fat tissue, the measured dielectric across the bandwidth varies from 5-15 that is theoretically acceptable, and the tumor tissue shows the dielectric in the range of 48-60 that matches the targeted specifications. Also, the conductivity curve for both tumor and fat tissue can be found in figure 7b where a good agreement is noticed between the measured and targeted values.

B. DIELECTRIC PROPERTIES OF HETEROGENEOUS PHANTOM

Table 5 shows the five (5) data samples of the dielectric properties of each layer of the heterogeneous phantom at five different positions. It is noticed that the mean value is close enough to the targeted value. Figure 8a and 8b

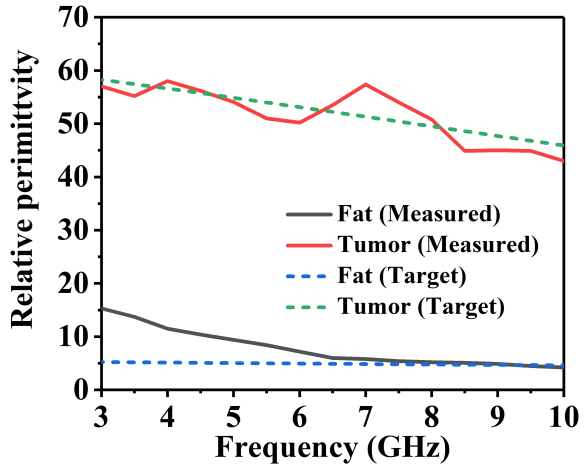

(a)

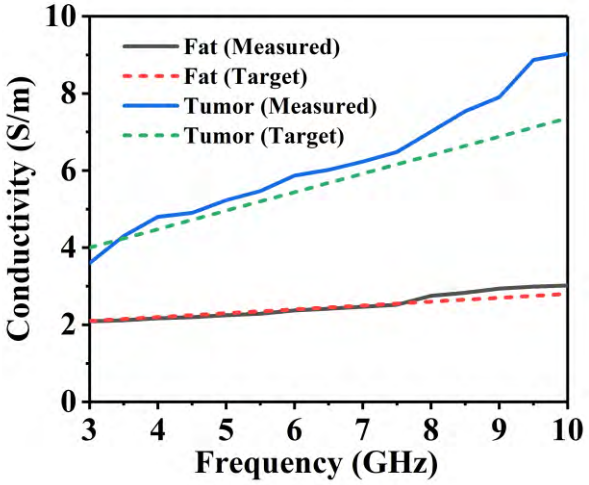

(b)

FIGURE 7. Dielectric properties of homogenous phantom: (a) Relative permittivity and (b) conductivity against frequency.

TABLE 5. Dielectric properties of the heterogeneous phantom.

Skin Layer						
Properties	Data 1	Data 2	Data 3	Data 4	Data 5	Mean
Permittivity ε_r	17.90	31.21	27.16	17.36	23.57 (center)	23.44
Loss tangent	-0.36	-0.23	-0.24	-0.34	-0.25	-0.28
Conductivity (S/m)	2.50	2.79	2.54	2.30	2.30	2.49
Fat Layer						
Permittivity ε_r	4.93	5.14	4.32	4.70	9.66 (center)	5.75
Loss tangent	-0.81	-0.78	-0.78	-0.75	-0.75	-0.77
Conductivity (S/m)	1.55	1.56	1.31	1.37	2.82	1.72
Glandular Layer						
Permittivity ε_r	19.31	12.84	18.08	12.35	16.18 (center)	15.75
Loss tangent	-0.39	-0.55	-0.54	-0.69	-0.56	-0.55
Conductivity (S/m)	2.93	2.75	3.80	3.32	3.53	3.27
Tumor Layer						
Permittivity ε_r	63.95	42.85	39.13	33.32	23.64 (center)	40.57
Loss tangent	-0.62	-0.34	-0.15	-0.40	-0.47	-0.40
Conductivity (S/m)	5.43	5.67	4.28	5.19	4.32	4.98

shows the relative permittivity or dielectric and conductivity against frequency. The skin layer has the dielectric of ranging 22-40 and conductivity of 1.5-2.5. The fatty tissue shows the dielectric of 5-15 and conductivity of 1.7-2.5. The gland tissue shows the dielectric of 15-45 and conductivity of 1.5-4, and for containing more watery content, the tumor tissue shows the maximum dielectric and conductivity. The dielectric for tumor is ranging from 35-56 and conductivity is 3.5-8.5 across the UWB band. All the results are identical to the desired specifications. Therefore, the work presented in this paper has the more realistic characteristics of the real human breast to be tested with the MBI system efficiency.

C. SAMPLE IMAGES GENERATED IN THE MBI SYSTEM USING THE PHANTOM SET

The results obtained from phantom measurement clearly resemble the standard results. The sample images generated from the same MBI experiment setup explained at [42], where backscattered signals are collected using a microwave antenna sensor and image constructed by applying Delay-and-Sum algorithms. The authors also applied rotation subtraction to remove the artifact. A mechanical rotating platform was used to collect the backscattering signals from the phantoms. A different set of data is obtained such as phantom without tumor and phantom with tumors. All the sample images of the stated scenarios are illustrated in figure 9 and 10. Fig 9(a) is mainly blank as expected because of the homogeneity of phantom A. Small insignificant specifications of noise appear at the top of phantom A probably because of cracks on its exterior. Fig 9(b) displays an individual point of high contrast to the fat materials as white along with some lower strength clutter below it. The high contrast location is regarded as the center of the tumor the clutter could be related to imperfect insertion of tumor leading to small cracks in the excess fat being filled up with tumor materials. Fig. 9(c) obviously shows two individual clutters indicating the existence of two tumors. Nevertheless, the top tumor in Fig 9(c) is slightly nearer to the center compared to the lower tumor. Upon re-exam of phantom, it had been mentioned that one tumor was positioned closer. The discrepancy could be seen

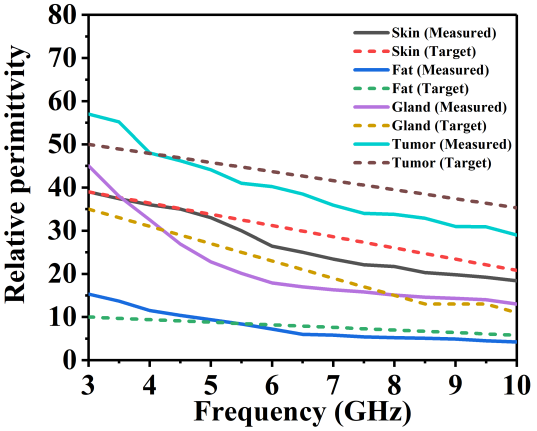

(a)

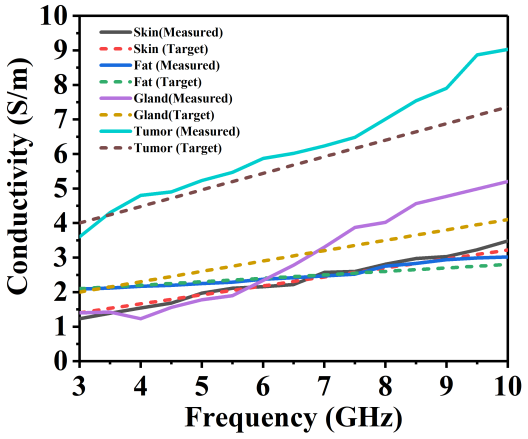

(b)

FIGURE 8. Dielectric properties of heterogeneous phantom: (a) relative permittivity and (b) conductivity against frequency.

in Fig 9(c). Finally, Fig 9(d) displays one high comparison clutter probably due to the tumor nearest to the skin. The additional three tumors also show up but just as low comparison clusters. Being that they are buried deeper, the reflected indicators face more attenuation, leading to less contrast. Nevertheless, the existence of four unique clutters indicates the recognition of most four tumors. The resolution of the images has been improved. For defining the deep penetration, more than one tumor in single phantom has been tested and the imaging results are presented in figure 9c and 9d. The primary imaging results of heterogenous phantom is illustrated in figure 10. Figure 10a represents the image without tumor inserted and several lighter clutters due to relatively higher dielectric of glandular tissue and figure 10b clearly indicate the presence to two tumors with dipper clutters. It is noticed that the level and shape of a conjecture of tumorous cells has a significant effect on the renovated images after analyzing the backscattering signals, which can be considered as the systematic evaluation of microwave breast imaging prototype systems.

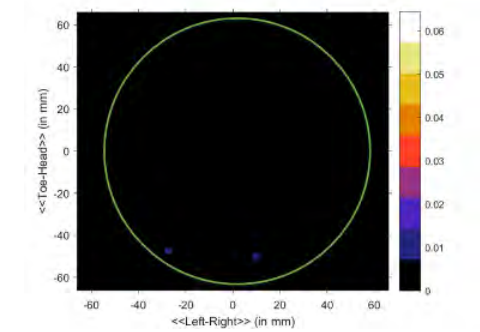

(a)

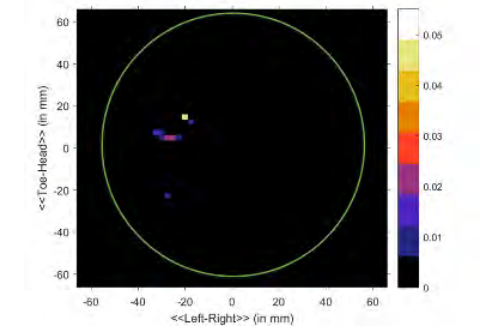

(b)

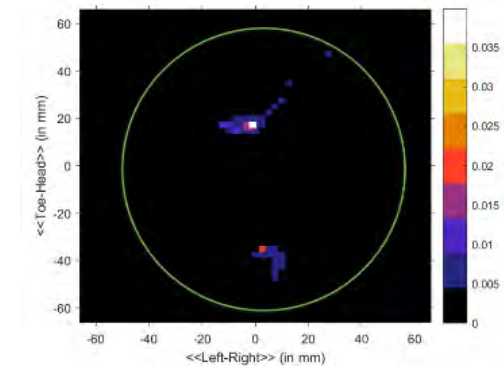

(c)

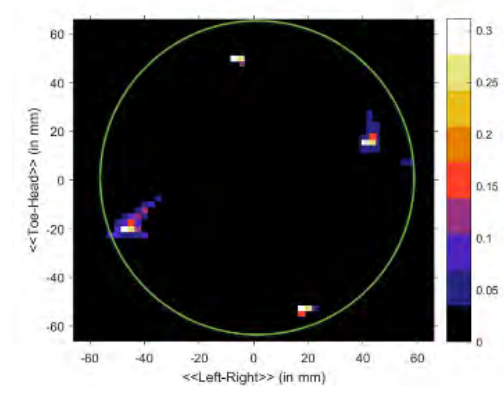

(d)

FIGURE 9. Primary Microwave Imaging results of homogeneous breast phantom (a) Phantom without tumor and, (b) Phantom with a tumor inside the phantom, (c) phantom with two tumors and (d) phantom with four tumors (deep purple indicates the tumor).

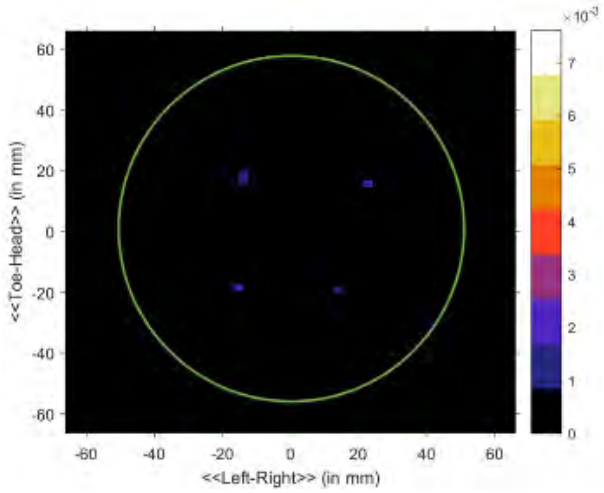

(a)

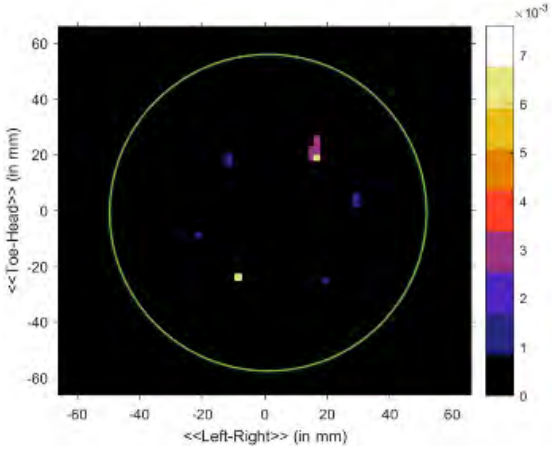

(b)

FIGURE 10. Primary Microwave Imaging results of heterogeneous breast phantom (a) Without tumor (b) With two tumors (deep yellow indicates the tumor).

V. CONCLUSION

The fabrication and measurement of medical breast phantoms and the evaluations of MBI systems using the prepared phantoms are presented in this paper. Two types of the phantom, homogenous and heterogeneous with several layers of tissues are fabricated separately, and complex anatomy of real like human breast is built. These breast phantoms can be used to produce a robust and flexible test platform for microwave tumor detection systems. The phantoms contain four layers of skin, fat, glandular and tumor that is suitable for hemispherical conformal imaging systems. The measurements of dielectric properties are listed and compared with the theoretical results to verify the phantom properties. The lifetime for the homogeneous is recorded as eight (8) weeks after proper preservation at the refrigerator, and heterogeneous phantoms hold its properties up to six (6) weeks, which is comparatively higher than the phantoms reported in the literature. Sample images generated from the scanning of the fabricated phantoms at different scenarios (multiple tumors with high-resolution image) in MBI systems also presented. Therefore, the phantoms can be a good substitute for testing before transferring to in vivo clinical testing.

REFERENCES

[1] T. Henriksson *et al.*, "Clinical trials of a multistatic UWB radar for breast imaging," in *Proc. Loughborough IEEE Antennas Propag. Conf. (LAPC)*, Nov. 2011, pp. 1–4.

[2] M. Kahar, A. Ray, D. Sarkar, and P. P. Sarkar, "An UWB microstrip monopole antenna for breast tumor detection," *Microw. Opt. Technol. Lett.*, vol. 57, no. 1, pp. 49–54, 2015.

[3] M. T. Islam, M. Samsuzzaman, M. N. Rahman, and M. T. Islam, "A compact slotted patch antenna for breast tumor detection," *Microw. Opt. Technol. Lett.*, vol. 60, no. 7, pp. 1600–1608, 2018.

[4] X. Li, S. K. Davis, S. C. Hagness, D. W. van der Weide, and B. D. Van Veen, "Microwave imaging via space-time beamforming: Experimental investigation of tumor detection in multilayer breast phantoms," *IEEE Trans. Microw. Theory Techn.*, vol. 52, no. 8, pp. 1856–1865, Aug. 2004.

[5] M. Klemm, I. J. Craddock, J. A. Leendertz, A. Preece, and R. Benjamin, "Radar-based breast cancer detection using a hemispherical antenna array—Experimental results," *IEEE Trans. Antennas Propag.*, vol. 57, no. 6, pp. 1692–1704, Jun. 2009.

[6] L. Wang, "Microwave sensors for breast cancer detection," *Sensors*, vol. 18, no. 2, p. 655, 2018.

[7] R. L. Siegel, K. D. Miller, and A. Jemal, "Cancer statistics, 2017," *CA, Cancer J. Clin.*, vol. 67, no. 1, pp. 7–30, 2017.

[8] W. T. Joines, R. L. Jirtle, M. D. Rafal, and D. J. J. Schaefer, "Microwave power absorption differences between normal and malignant tissue," *Int. J. Radiat. Oncol. Biol. Phys.*, vol. 6, no. 6, pp. 681–687, 1980.

[9] K. D. Paulsen, P. M. Meaney, L. Gilman, and L. C. Gilman, *Alternative Breast Imaging: Four Model-Based Approaches*. Springer, 2005.

[10] C.-C. Chen, Y.-L. Wan, Y.-Y. Wai, and H.-L. Liu, "Quality assurance of clinical MRI scanners using ACR MRI phantom: Preliminary results," *J. Digit. Imag.*, vol. 17, no. 4, pp. 279–284, 2004.

[11] P. M. Meaney, C. J. Fox, S. D. Geimer, and K. D. Paulsen, "Electrical characterization of glycerin: Water mixtures: Implications for use as a coupling medium in microwave tomography," *IEEE Trans. Microw. Theory Techn.*, vol. 65, no. 5, pp. 1471–1478, May 2017.

[12] A. Santorelli, O. Laforest, E. Porter, and M. Popović, "Image classification for a time-domain microwave radar system: Experiments with stable modular breast phantoms," in *Proc. IEEE 9th Eur. Conf. Antennas Propag. (EuCAP)*, Apr. 2015, pp. 1–5.

[13] N. Joachimowicz, C. Conessa, T. Henriksson, and B. Duchêne, "Breast phantoms for microwave imaging," *IEEE Antennas Wireless Propag. Lett.*, vol. 13, pp. 1333–1336, 2014.

[14] H. Woodard and D. R. White, "The composition of body tissues," *The Brit. J. Radiol.*, vol. 59, no. 708, pp. 1209–1218, 1986.

[15] T. Sugitani *et al.*, "Complex permittivities of breast tumor tissues obtained from cancer surgeries," *Appl. Phys. Lett.*, vol. 104, no. 25, p. 253702, 2014.

[16] M. J. Burfeindt *et al.*, "MRI-derived 3-D-printed breast phantom for microwave breast imaging validation," *IEEE Antennas Wireless Propag. Lett.*, vol. 11, pp. 1610–1613, 2012.

[17] N. Joachimowicz, B. Duchêne, C. Conessa, and O. Meyer, "Easy-to-produce adjustable realistic breast phantoms for microwave imaging," in *Proc. IEEE 10th Eur. Conf. Antennas Propag. (EuCAP)*, Apr. 2016, pp. 1–4.

[18] D. R. Herrera, T. Reimer, M. S. Nepote, and S. Pistorius, "Manufacture and testing of anthropomorphic 3D-printed breast phantoms using a microwave radar algorithm optimized for propagation speed," in *Proc. IEEE 11th Eur. Conf. Antennas Propag. (EUCAP)*, Mar. 2017, pp. 3480–3484.

[19] M. Lazebnik, E. L. Madsen, G. R. Frank, and S. C. Hagness, "Tissue-mimicking phantom materials for narrowband and ultrawideband microwave applications," *Phys. Med. Biol.*, vol. 50, no. 18, p. 4245, Oct. 2005.

[20] S. Romeo *et al.*, "Dielectric characterization study of liquid-based materials for mimicking breast tissues," *Microw. Opt. Technol. Lett.*, vol. 53, no. 6, pp. 1276–1280, 2011.

[21] M. T. Islam, M. Z. Mahmud, N. Misran, J.-I. Takada, and M. Cho, "Microwave breast phantom measurement system with compact side slotted directional antenna," *IEEE Access*, vol. 5, pp. 5321–5330, 2017.
[22] D. Vrba, J. Vrba, D. B. Rodrigues, and P. Stauffer, "Numerical investigation of novel microwave applicators based on zero-order mode resonance for hyperthermia treatment of cancer," *J. Franklin Inst.*, vol. 354, no. 18, pp. 8734–8746, 2017.
[23] D. Vrba and J. Vrba, "Novel applicators for local microwave hyperthermia based on zeroth-order mode resonator metamaterial," *Int. J. Antennas Propag.*, vol. 2014, Apr. 2014, Art. no. 631398.
[24] A. W. Guy, "Analyses of electromagnetic fields induced in biological tissues by thermographic studies on equivalent phantom models," *IEEE Trans. Microw. Theory Techn.*, vol. MTT-16, no. 2, pp. 205–214, Feb. 1971.
[25] T. Ishida and H. Kato, "Muscle equivalent agar phantom for 13.56 MHz RF-induced hyperthermia," *J. Med. Sci.*, vol. 4, no. 2, pp. 134–140, 1980.
[26] A. Dabbagh, B. J. J. Abdullah, C. Ramasindarum, and N. H. A. Kasim, "Tissue-mimicking gel phantoms for thermal therapy studies," *Ultrason. Imag.*, vol. 36, no. 4, pp. 291–316, Mar. 2014.
[27] A. Mashal, F. Gao, and S. C. Hagness, "Heterogeneous anthropomorphic phantoms with realistic dielectric properties for microwave breast imaging experiments," *Microw. Opt. Technol. Lett.*, vol. 53, no. 8, pp. 1896–1902, Aug. 2011.
[28] B. L. Oliveira, A. Shahzad, M. O'Halloran, R. C. Conceição, M. Glavin, and E. Jones, "Combined breast microwave imaging and diagnosis system," in *Proc. Prog. Electromagn. Res. Symp.*, Prague, Czech Republic, 2015, pp. 6–9.
[29] B. L. Oliveira, M. O'Halloran, R. C. Conceição, M. Glavin, and E. Jones, "Development of clinically informed 3-D tumor models for microwave imaging applications," *IEEE Antennas Wireless Propag. Lett.*, vol. 15, pp. 520–523, 2016.
[30] M. Lazebnik *et al.*, "A large-scale study of the ultrawideband microwave dielectric properties of normal breast tissue obtained from reduction surgeries," *Phys. Med. Biol.*, vol. 52, no. 10, pp. 2637–2656, 2007.
[31] M. Lazebnik, M. Okoniewski, J. H. Booske, and S. C. Hagness, "Highly accurate Debye models for normal and malignant breast tissue dielectric properties at microwave frequencies," *IEEE Microw. Wireless Compon. Lett.*, vol. 17, no. 12, pp. 822–824, Dec. 2007.
[32] M. Lazebnik *et al.*, "A large-scale study of the ultrawideband microwave dielectric properties of normal, benign and malignant breast tissues obtained from cancer surgeries," *Phys. Med. Bio.*, vol. 52, no. 20, p. 6093, Oct. 2007.
[33] P. M. Meaney, M. W. Fanning, D. Li, S. P. Poplack, and K. D. Paulsen, "A clinical prototype for active microwave imaging of the breast," *IEEE Trans. Microw. Theory Techn.*, vol. 48, no. 11, pp. 1841–1853, Nov. 2000.
[34] E. C. Fear, J. Bourqui, C. Curtis, D. Mew, B. Docktor, and C. Romano, "Microwave breast imaging with a monostatic radar-based system: A study of application to patients," *IEEE Trans. Microw. Theory Techn.*, vol. 61, no. 5, pp. 2119–2128, May 2013.
[35] A. W. Preece, I. J. Craddock, M. Shere, L. Jones, and H. L. Winton, "MARIA M4: Clinical evaluation of a prototype ultrawideband radar scanner for breast cancer detection," *J. Med. Imag.*, vol. 3, no. 3, p. 033502, 2016.
[36] E. Porter, J. Fakhoury, R. Oprisor, M. Coates, and M. Popović, "Improved tissue phantoms for experimental validation of microwave breast cancer detection," in *Proc. IEEE 4th Eur. Conf. Antennas Propag. (EuCAP)*, Apr. 2010, pp. 1–5.
[37] J. Garrett and E. Fear, "A new breast phantom with a durable skin layer for microwave breast imaging," *IEEE Trans. Antennas Propag.*, vol. 63, no. 4, pp. 1693–1700, Apr. 2015.
[38] S. Seewattanapon and P. Akkaraekthalin, "A broadband complex permittivity probe using stepped coaxial line," *J. Electromagn. Anal. Appl.*, vol. 3, no. 8, p. 312, 2011.
[39] P. M. Meaney, A. P. Gregory, N. R. Epstein, and K. D. Paulsen, "Microwave open-ended coaxial dielectric probe: Interpretation of the sensing volume re-visited," *BMC Med. Phys.*, vol. 14, no. 1, p. 3, 2014.
[40] N. Piladaeng, N. Angkawisittpan, and S. Homwuttiwong, "Determination of relationship between dielectric properties, compressive strength, and age of concrete with rice husk ash using planar coaxial probe," *Meas. Sci. Rev.*, vol. 16, no. 1, pp. 14–20, 2016.
[41] E. A. Alwan, A. Kiourti, and J. L. Volakis, "Indium tin oxide film characterization at 0.1–20 GHz using coaxial probe method," *IEEE Access*, vol. 3, pp. 648–652, 2015.
[42] M. T. Islam, M. Samsuzzaman, M. Islam, S. Kibria, and M. J. Singh, "A homogeneous breast phantom measurement system with an improved modified microwave imaging antenna sensor," *Sensors*, vol. 18, no. 9, p. 2962, 2018.

MD TARIKUL ISLAM was born in Patuakhali, Bangladesh, in 1994. He received the B.Sc. degree in computer science and engineering from the Patuakhali Science and Technology University, in 2016. He is currently pursuing the master's degree with the Universiti Kebangsaan Malaysia (UKM), Malaysia. He is also a Graduate Research Assistant with the Department of Electrical, Electronic and Systems Engineering, UKM. He has authored or co-authored a number of referred journals and conference papers. His research interests include communication antenna design, wireless communication, RF engineering, and microwave imaging.

MD SAMSUZZAMAN was born in Jhenaidah, Bangladesh, in 1982. He received the B.Sc. and M.Sc. degrees in computer science and engineering from Islamic University Kushtia, Bangladesh, in 2005 and 2007, respectively, and the Ph.D. degree from Universiti Kebangsaan Malaysia, Malaysia, in 2015. From 2008 to 2011, he was a Lecturer with the Patuakhali Science and Technology University (PSTU), Bangladesh, where he was an Assistant Professor with the Patuakhali Science and Technology University, from 2011 to 2015. He is currently an Associate Professor with PSTU. He is also a Post-Doctoral Fellow with Universiti Kebangsaan Malaysia. He has authored or co-authored over 80 research journal articles, nearly 20 conference articles, and a few book chapters on various topics related to antennas, microwaves, and electromagnetic radiation analysis with one inventory patents filed. His Google scholar citation is 546 and H-index is 13. His research interests include communication antenna design, satellite antennas, and microwave imaging.

SALEHIN KIBRIA was born in Dhaka, Bangladesh, in 1988. He received the B.Eng. degree (Hons.) in telecommunications from Universiti Kebangsaan Malaysia, Malaysia, and the M.Sc. degree (Hons.) in electronics from Multimedia University. He is currently pursuing the Ph.D. degree with Universiti Kebangsaan Malaysia. He was employed as a Research Assistant at the Faculty of Engineering and Built Environment in a research Project funded by the Malaysian Government. His research interests focuse on microwave imaging, RFID systems, and heuristic optimization techniques.

MOHAMMAD TARIQUL ISLAM is currently a Professor with the Department of Electrical, Electronic and Systems Engineering, Universiti Kebangsaan Malaysia (UKM), and a Visiting Professor of the Kyushu Institute of Technology, Japan. He has the authored or co-authored over 350 research journal articles, nearly 165 conference articles, and a few book chapters on various topics related to antennas, microwaves, and electromagnetic radiation analysis with 16 inventory patents filed. His publications have been cited 4210 times and his H-index is 33 (Source: Scopus). His Google scholar citation is 5545 and H-index is 36. He was a recipient of more than 40 research grants from the Malaysian Ministry of Science, Technology and Innovation, Ministry of Education, UKM Research Grant, international research grants from Japan and Saudi Arabia. His research interests include communication antenna design, radio astronomy antennas, satellite antennas, and electromagnetic radiation analysis. He is a Chartered Professional Engineer and a member of the IET, U.K., and the IEICE, Japan. He currently serves as the Editor-in-Chief for the *International Journal of Electronics* and *Informatics*, and an Associate Editor for *Electronics Letter*. He received several international gold medal awards, the Best Invention in Telecommunication Award, a special award from Vietnam for his research and innovation, and the Best Researcher Award in 2010 and 2011 at UKM. He also received the Best Innovation Award in 2011 and the Best Research Group in ICT niche from UKM, in 2014. He was a recipient of the Best Paper Presentation Award in the 2012 International Symposium on Antennas and Propagation, Nagoya, Japan, and the 2015 in IconSpace Conference, and the Publication Award from the Malaysian Space Agency in 2009, 2010, 2013, and 2014.